Inorganic Chemistry
Article

Inorg. Chem. **2009**, *48*, 5779–5789 **5779**
DOI: 10.1021/ic900105u

Electronic Structure and Spin Exchange Interactions in $Na_2V_3O_7$: a Vanadium(IV) Oxide Nanotubular Phase

Antonio Rodríguez-Fortea,*,† Miquel Llunell,*,‡ Pere Alemany,‡ and Enric Canadell§

†*Departament de Química Física i Inorgànica, Universitat Rovira i Virgili, Marcel·lí Domingo s/n, 43007 Tarragona, Spain,* ‡*Departament de Química Física and Institut de Química Teòrica i Computacional (IQTCUB), Universitat de Barcelona, Diagonal 647, 08028 Barcelona, Spain, and* §*Institut de Ciència de Materials de Barcelona (CSIC), Campus de la UAB, 08193 Bellaterra, Spain*

Received January 19, 2009

The electronic structure of the inorganic nanotubular phase $Na_2V_3O_7$ has been studied by means of first-principles DFT calculations. The magnetic behavior in this system is relatively complex to study because there are as many as 30 different exchange interactions in the unit cell. The coupling constants are computed directly from the energy differences of several spin configurations. It is found that because of the special geometry of the nanotube, the nearest-neighbor coupling constants are not the only important ones and other next-nearest-neighbor constants cannot be neglected. In contrast with previous studies, it is found that at least 12 different coupling constants must be considered to correctly describe the spin arrangement in this system. However, to get more meaningful values for the smaller constants, a larger set of at least 17 constants must be explicitly taken into account. The lowest-energy collinear spin configuration is found to exhibit ferromagnetic coupling between the rings of the nanotube, whereas the coupling can be ferro- or antiferromagnetic within those rings. This leads to two important spin-frustrated interactions. Use of the so-called dimer approximation (i.e., substituting 16 paramagnetic V(IV) ions of the nanotube by 16 diamagnetic Ti(IV) ions, thus keeping the total charge of the system constant and leaving only two magnetic centers) is found to give invaluable hints concerning the nature of the magnetic interactions. This procedure may be helpful to analyze the magnetic properties of similar non-trivial systems with many paramagnetic centers.

Introduction

$Na_2V_3O_7$[1] is a remarkable material at the crossroads of two of the more challenging streams in modern materials science: nanoscience and low-dimensional magnetism. Although inorganic nanotubes had been known for some time,[2] $Na_2V_3O_7$ was the first transition-metal-oxide based nanotubular system to be described. Since the vanadium atoms are in a d^1 configuration, the study of the magnetic behavior of such an array of $S = 1/2$ centers is very appealing. As it is well-known,[3,4] many low-dimensional quantum spin systems exhibit an unconventional behavior. For instance, both theoretical predictions and experimental studies concerning one-dimensional spin arrays like spin-ladders have uncovered hand-in-hand the unexpected and unusual properties of such systems. The number of legs (n) of the ladder largely determines their physical behavior. A spin $S = 1/2$ ladder with antiferromagnetic (AF) interactions is expected to exhibit a gap in the spin excitations spectrum if it has an even number of legs. However, no gap is expected if the number of legs is odd. In addition, it has been proposed that the short-range AF spin correlations should lead to superconductivity when a small number of carriers are doped into even leg ladders. The experimental observation of gapped and gapless ground states for $SrCu_2O_3$ ($n = 2$) and $Sr_2Cu_3O_5$ ($n = 3$),[5] respectively, have been taken as experimental realizations of the first prediction. The raising of superconductivity under high pressure in $(Sr, Ca)_{14}Cu_{24}O_{41+x}$ ($n = 2$)[6] has been suggested to be a confirmation of the second. However, even after intense activity there are still aspects of the spin-ladder behavior which are not yet well

*To whom correspondence should be addressed. E-mail: antonio.rodriguezf@urv.cat (A.R.-F.), llunell@ub.edu (M. Ll). Phone: +34 977 558181 (A.R.-F.), +34 93 403 9289 (M. Ll). Fax: +34 977 559 563 (A.R.-F.), +34 93 402 1231 (M. Ll).

(1) Millet, P.; Henry, J. Y.; Mila, F.; Galy, J. *J. Solid State Chem.* **1999**, *147*, 676.
(2) Tenne, R.; Margulis, L.; Genut, M.; Hodes, G. *Nature*. **1992**, *360*, 444.
(3) (a) Dagotto, E.; Rice, T. M. *Science* **1996**, *271*, 618. (b) Dagotto, E. *Rep. Prog. Phys.* **1999**, *62*, 1525.
(4) Lemmens, P.; Güntherodt, G.; Gros, C. *Phys. Rep.* **2003**, *375*, 1.
(5) (a) Azuma, M.; Hiroi, M.; Takano, M.; Ishida, K.; Kitaoka, Y. *Phys. Rev. Lett.* **1994**, *73*, 3463. (b) Kojima, K.; Keren, A.; Luke, G. M.; Nachumi, B.; Wu, W. D.; Uemura, Y. J.; Azuma, M.; Takano, M. *Phys. Rev. Lett.* **1995**, *74*, 2812.
(6) (a) Uehara, M.; Nagata, T.; Akimitsu, J.; Takahashi, H.; Mori, N.; Kinoshita, K. *J. Phys. Soc. Jpn.* **1996**, *65*, 2764. (b) Vuletic, T.; Korin-Hamzic, B.; Ivek, T.; Tomic, S.; Gorshunov, B.; Dressel, M.; Akimitsu, J. *Phys. Rep.* **2006**, *428*, 169.

Published on Web 05/29/2009

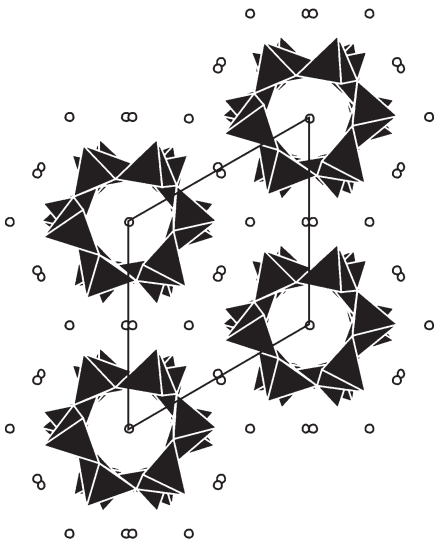

Figure 1. Projection of the crystal structure of $Na_2V_3O_7$ along the *c*-direction.

understood. For instance, it is not completely clear how the existence of periodic boundary conditions along the rung may affect the predictions concerning the spin excitation spectrum.[7]

Even if a relatively large variety of materials has been considered, the experimental work concerning spin-ladders has concentrated on cuprates and vanadates. The synthesis of $Na_2V_3O_7$ by Millet and co-workers[1] came as an interesting addition to this literature because this material can be considered as a spin 1/2 ladder with odd legs and with periodicity in the rung direction so that it is a useful material allowing to test theoretical predictions. The crystal structure of $Na_2V_3O_7$ is schematically shown in Figure 1: it is an hexagonally packed array of $V_3O_7^{2-}$ nanotubes separated by sodium cations that provide cohesion to the structure. Additional sodium atoms are found in the channels inside the nanotubes (see a detailed structural description below). The structural features of this phase are such that no relevant interaction between magnetic centers of different nanotubes can occur (see below for the three-dimensional electronic structure calculated for this system which provides further evidence for this fact). Thus, in understanding the magnetic behavior of $Na_2V_3O_7$, one may focus on a single nanotube. This material has been the objective of several works measuring its optical and magnetic properties,[8−14] and it turns out that the reported magnetic properties of $Na_2V_3O_7$ do not fit with the predictions for odd leg spin-ladders.

The puzzle that this system puts forward has motivated several theoretical studies of its electronic structure and spin exchange interactions.[15−18] In particular, Whangbo and Koo[15] studied the relative magnitudes of the spin exchange interactions in the nanotube by means of an extended Hückel-based spin dimer analysis and concluded that the magnetic behavior of the system can be described by six mutually intersecting helical chains. Later, Saha-Dasgupta et al.[16] presented a detailed ab initio microscopic analysis of the electronic and magnetic properties of this system based on Density Functional Theory (DFT) band structure calculations using the linearized-muffin-tin-orbital (LMTO) and the linear augmented plane wave (LAPW) methods. They derived a model Hamiltonian in a first-principles manner by means of the downfolding technique and computed the hopping integrals (t_{ij}) for different pairs of V(IV) paramagnetic centers. According with the computed values of the hopping integrals, they fitted the experimental magnetic susceptibility using a Heisenberg Hamiltonian using only two exchange coupling constants (J_{ij}) within the rings and neglecting all inter-ring couplings. Large antiferromagnetic couplings were predicted for edge-sharing, as well as for corner-sharing, V−V interactions within the ring. More recently, Mazurenko et al.[17] have performed first-principles calculations of the electronic structure and exchange couplings for this compound by means of the Local Density Approximation Hubbard parameter U approach (LDA + U).[18] These authors took into account the nine exchange coupling constants between nearest neighbor V(IV) centers and computed them following the first-principles Green function method.[19] They found that the intra-ring exchange couplings are mainly antiferromagnetic, but the inter-ring couplings are ferromagnetic and of the same order of magnitude. This short overview makes clear that the magnetic behavior of this nanotubular phase still lacks a firm theoretical understanding. It is our purpose here to reconsider in detail this system to (a) determine the minimal set of coupling constants which any model trying to rationalize the experimental measurements must take into account, and (b) provide reliable values for these coupling constants.

Our experience in the theoretical prediction of exchange coupling constants for polynuclear compounds,[20−25] as well as for extended systems,[26,27] let us claim that the indirect evaluation of coupling constants may lead in the best

(7) (a) Schulz, H. J. In *Correlated Fermions and Transport in Mesoscopic Systems*; Martin, T., Montambaux, G., Tran Than Van, J., Eds.; Editions Frontières: Gif-sur-Yvette, **1996**; p 81. (b) Kawano, K.; Takahashi, M. *J. Phys. Soc. Jpn.* **1997**, *66*, 4001. (c) Wang, H.-T. *Phys. Rev. B* **2001**, *64*, 174410.

(8) Gavilano, J. L.; Rau, D.; Mushkolaj, S.; Ott, H. R.; Millet, P.; Mila, F. *Physica B* **2002**, *312−313*, 622.

(9) Choi, J.; Musfeldt, J. L.; Wang, Y. J.; Koo, H.-J.; Whangbo, M.-H.; Galy, J.; Millet, P. *Chem. Mater.* **2002**, *14*, 924.

(10) Gavilano, J. L.; Rau, D.; Mushkolaj, S.; Ott, H. R.; Millet, P.; Mila, F. *Phys. Rev. Lett.* **2003**, *90*, 167202.

(11) Gavilano, J. L.; Rau, D.; Mushkolaj, S.; Ott, H. R.; Mila, F.; Millet, P. *Physica B* **2003**, *329−333*, 703.

(12) Gavilano, J. L.; Felder, E.; Rau, D.; Ott, H. R.; Millet, P.; Mila, F.; Cichorek, T.; Mota, A. C. *Phys. Rev. B* **2005**, *72*, 064431.

(13) Gavilano, J. L.; Felder, E.; Rau, D.; Ott, H. R.; Millet, P.; Mila, F.; Cichorek, T.; Mota, A. C. *Physica B* **2005**, *378−380*, 123.

(14) Vertesi, T.; Bene, E. *Phys. Rev. B* **2006**, *73*, 134404.

(15) Whangbo, M.-H.; Koo, H.-J. *Solid State Commun.* **2000**, *115*, 675.

(16) Saha-Dasgupta, T.; Valentí, R.; Capraro, F.; Gros, C. *Phys. Rev. Lett.* **2005**, *95*, 107201.

(17) Mazurenko, V. V.; Mila, F.; Anisimov, V. I. *Phys. Rev. B* **2006**, *73*, 014418.

(18) Anisimov, V. I.; Zaanen, J.; Andersen, O. K. *Phys. Rev. B* **1991**, *44*, 943.

(19) Liechtenstein, A. I.; Anisimov, V. I.; Zaanen, J. *Phys. Rev. B* **1995**, *52*, R5467.

(20) Rodriguez-Fortea, A.; Alemany, P.; Alvarez, S.; Ruiz, E. *Chem.—Eur. J.* **2001**, *7*, 627.

(21) Rodriguez-Fortea, A.; Ruiz, E.; Alemany, P.; Alvarez, S. *Monatsh. Chem.* **2003**, *134*, 307.

(22) Rodriguez-Fortea, A.; Alemany, P.; Alvarez, S.; Ruiz, E. *Eur. J. Inorg. Chem.* **2004**, 143.

(23) Rodriguez-Fortea, A.; Ruiz, E.; Alvarez, S.; Alemany, P. J. *Chem. Soc., Dalton Trans* **2005**, 2624.

(24) Tercero, J.; Ruiz, E.; Alvarez, S.; Rodriguez-Fortea, A.; Alemany, P. *J. Mater. Chem.* **2006**, *16*, 2729.

(25) Ruiz, E.; Rodriguez-Fortea, A.; Cano, J.; Alvarez, S.; Alemany, P. *J. Comput. Chem.* **2003**, *24*, 982.

(26) Ruiz, E.; Llunell, M.; Cano, J.; Rabu, P.; Drillon, M.; Massobrio, C. *J. Phys. Chem. B* **2006**, *110*, 115.

(27) (a) Ruiz, E.; Llunell, M.; Alemany, P. *J. Solid State Chem.* **2003**, *176*, 400. (b) Ruiz, E. *Struct. Bonding (Berlin)* **2004**, *113*, 71.

situations to a qualitative agreement with experimental results. Quantitative results may only be obtained by means of direct computation of several spin states of the system, at least one spin state more than the number of coupling constants to be computed. The most precise methods to compute coupling constants are the ab initio wave function-based methods that include electron correlation, namely CASPT2 and DDCI,[28−30] but their use is limited to medium-size systems with few paramagnetic centers and a small number of unpaired electrons. Methods based on DFT combined with the broken-symmetry approximation[31] offer an excellent alternative for the computation of exchange coupling constants in medium-size polynuclear compounds[25,32−36] and the simplest alternative for large-size polynuclear compounds or even for extended systems.[26,27,37−39] It is well-known that LDA overestimates the antiferromagnetic character of the exchange coupling interactions while the Generalized Gradient Approximation (GGA), in general, correctly predicts the nature of the coupling, except for some cases in which the coupling constants are very small, even if the antiferromagnetic interactions are somewhat overestimated. The best performance so far is provided by hybrid functionals, as for example B3LYP, in combination with Gaussian basis sets, which allows for a very good prediction of exchange coupling constants. However, its use is limited to medium-size polynuclear complexes and periodic systems with a moderate number of paramagnetic centers per unit cell. For large-size polynuclear complexes and periodic systems with a large number of paramagnetic centers per repeat unit, the use of GGA functionals, in particular that proposed by Perdew−Burke−Ernzerhof (PBE), together with a numerical basis set provides a good compromise between accuracy and computational requirements, being usually the only practical approach to tackle the problem.[38−40]

In the following we report a theoretical DFT-based study of the electronic structure and spin exchange interactions in $Na_2V_3O_7$ which we believe is the most complete analysis of the nature of the magnetic interactions in this complex material. The peculiar structure of this nanotubular system which possesses 18 V(IV) paramagnetic centers per repeat unit, and in which the V(IV) ions are not that far from their next-nearest neighbors (NNN), make us suspect that some NNN V−V interactions can play an important role in the magnetic behavior of this system and thus the previous studies may suffer from this shortcoming. Therefore, we include a priori in our study the 30 different coupling constants that can be defined within the unit cell. We believe that the present study provides a precise evaluation of the different magnetic interactions in $Na_2V_3O_7$, thus opening the way toward a detailed understanding of its electronic structure and spin exchange interactions, and gives useful hints concerning the analysis of spin exchange interactions in nanotubular systems.

Computational Details

The first-principles spin-polarized calculations for $Na_2V_3O_7$ and some titanium substituted models (see below) were carried out using a numerical atomic orbitals DFT approach,[41] which was developed for efficient calculations in large systems and implemented in the SIESTA code.[42−44] We have used the generalized gradient approximation to DFT and, in particular, the functional of Perdew, Burke, and Ernzerhof.[45] Only the valence electrons are considered in the calculation, with the core being replaced by norm-conserving scalar relativistic pseudopotentials[46] factorized in the Kleinman−Bylander form.[47] Non-linear partial core corrections to describe the exchange and correlations in the core region were used for V and Ti.[48] We have used a split-valence triple-ζ basis set including polarization orbitals for V, Ti, and O and a split-valence double-ζ basis set including polarization orbitals for Na, as obtained with an energy shift of 50 meV.[49] The energy cutoff of the real space integration mesh was 150 Ry and the Brillouin zone was sampled using a grid of $(2 \times 2 \times 3)$ k-points.[50] The experimental crystal structure was used in all calculations.

Since a detailed description of the computational strategy used to calculate the exchange coupling constants in polynuclear complexes is outside the scope of this article, we will limit our discussion here to its most relevant aspects. Previously, a series of papers devoted to such a purpose have been published.[25,32] The spin Hamiltonian for a general polynuclear complex without anisotropic terms can be expressed as

$$\hat{H} = -\sum_{i>j} J_{ij}\hat{S}_i\hat{S}_j \qquad (1)$$

where $\hat{S}_i$ and $\hat{S}_j$ are the spin operators of the paramagnetic centers i and j and the J_{ij} parameters are the exchange

(28) Queralt, N.; De Graaf, C.; Cabrero, J.; Caballol, R. *Mol. Phys.* **2003**, *101*, 2095.
(29) Queralt, N.; Taratiel, D.; de Graaf, C.; Caballol, R.; Cimiraglia, R.; Angeli, C. *J. Comput. Chem.* **2008**, *29*, 994.
(30) Cabrero, J.; de Graaf, C.; Bordas, E.; Caballol, R.; Malrieu, J. P. *Chem.—Eur. J.* **2003**, *9*, 2307.
(31) (a) Noodleman, L. *J. Chem. Phys.* **1981**, *74*, 5737. (b) Noodleman, L.; Case, D. A. *Adv. Inorg. Chem.* **1992**, *38*, 423.
(32) (a) Ruiz, E.; Alemany, P.; Alvarez, S.; Cano, J. *J. Am. Chem. Soc.* **1997**, *119*, 1297. (b) Ruiz, E.; Alvarez, S.; Cano, J.; Polo, V. *J. Chem. Phys.* **2005**, *123*, 164110.
(33) Ruiz, E.; Cano, J.; Alvarez, S.; Alemany, P. *J. Comput. Chem.* **1999**, *20*, 1391.
(34) Cauchy, T.; Ruiz, E.; Alvarez, S. *J. Am. Chem. Soc.* **2006**, *128*, 15722.
(35) Desplanches, C.; Ruiz, E.; Rodriguez-Fortea, A.; Alvarez, S. *J. Am. Chem. Soc.* **2002**, *124*, 5197.
(36) (a) Valero, R.; Costa, R.; Moreira, I. d. P. R.; Truhlar, D. G.; Illas, F. *J. Chem. Phys.* **2008**, *128*, 114103. (b) Moreira, I. d. P. R.; Illas, F. *Phys. Chem. Chem. Phys.* **2006**, *8*, 1645. (c) Illas, F.; Moreira, I. d. P. R.; de Graaf, C.; Barone, V. *Theor. Chem. Acc.* **2000**, *104*, 265. (d) Bencini, A.; Totti, F.; Daul, C. A.; Doclo, K.; Fantucci, P.; Barone, V. *Inorg. Chem.* **1997**, *36*, 5022. (e) Adamo, C.; Barone, V.; Bencini, A.; Totti, F.; Ciofini, I. *Inorg. Chem.* **1999**, *38*, 1996.
(37) Cano, J.; Costa, R.; Alvarez, S.; Ruiz, E. *J. Chem. Theor. Comput.* **2007**, *3*, 782.
(38) Ruiz, E.; Rodriguez-Fortea, A.; Cano, J.; Alvarez, S. *J. Phys. Chem. Sol.* **2004**, *65*, 799.
(39) Ruiz, E.; Cauchy, T.; Cano, J.; Costa, R.; Tercero, J.; Alvarez, S. *J. Am. Chem. Soc.* **2008**, *130*, 7420.
(40) Ruiz, E.; Cano, J.; Alvarez, S.; Gouzerh, P.; Verdaguer, M. *Polyhedron* **2007**, *26*, 2161.
(41) (a) Hohenberg, P.; Kohn, W. *Phys. Rev.* **1964**, *136*, B864. (b) Kohn, W.; Sham, L. J. *Phys. Rev.* **1965**, *140*, A1133.
(42) Soler, J. M.; Artacho, E.; Gale, J. D.; García, A.; Junquera, J.; Ordejón, P.; Sánchez-Portal, D. *J. Phys.: Condens. Matter* **2002**, *14*, 2745.
(43) http://www.uam.es/siesta/
(44) For a review on applications of the SIESTA approach in materials science see: Sánchez-Portal, D.; Ordejón, P.; Canadell, E. *Struct. Bonding (Berlin)* **2004**, *113*, 103.
(45) Perdew, J. P.; Burke, K.; Ernzerhof, M. *Phys. Rev. Lett.* **1996**, *77*, 3865.
(46) Troullier, N.; Martins, J. L. *Phys. Rev. B* **1991**, *43*, 1993.
(47) Kleinman, L.; Bylander, D. M. *Phys. Rev. Lett.* **1982**, *48*, 1425.
(48) Louie, S. G.; Froyen, S.; Cohen, M. L. *Phys. Rev. B* **1982**, *26*, 1738.
(49) Artacho, E.; Sánchez-Portal, D.; Ordejón, P.; García, A.; Soler, J. M. *Phys. Stat. Sol. (b)* **1999**, *215*, 809.
(50) Monkhorst, H. J.; Park, J. D. *Phys. Rev. B* **1976**, *13*, 5188.

coupling constants for the different pairwise interactions between the paramagnetic centers of the compound. For dinuclear compounds, it has been found that, when using DFT-based wave functions, reasonable estimates of the exchange coupling constants can be obtained from the energy difference between the low spin configuration, E_{LS} (the traditionally called broken-symmetry solution for symmetric complexes), and the configuration with the highest spin, E_{HS}, by means of the following equation

$$J = \frac{E_{LS} - E_{HS}}{2S_1S_2 + S_2} \quad (2)$$

This solution, which corresponds to the non-projected approach, usually provides good results because the self-interaction error, which is present in the commonly used exchange-correlation functionals, incorporates some amount of static correlation. As a result, the energy corresponding to the single-determinant low spin wave function is a good approximation to that of the low spin state.[32b] The use of the alternative spin projected approach, as proposed originally by Noodlemann,[31] usually results in an overestimation of the calculated J values, specially for complexes with paramagnetic centers with low S_i values as for example $S = 1/2$ Cu(II) cations.[36]

For the evaluation of the n different coupling constants J_{ij} present in a polynuclear complex, we need to carry out calculations for at least $n + 1$ different spin distributions. Thus, solving the system of n equations obtained from the energy differences we can obtain the n coupling constants.[25] In the case that more than $n + 1$ spin distributions were calculated, a fitting procedure to obtain the coupling constants must be used.[27b] However, the sensitivity of the calculated J_{ij} values to the number of spin distributions employed in the calculation is usually rather weak.

Results and Discussion

Crystal Structure. As shown in Figure 1, $Na_2V_3O_7$ is built from V_3O_7 nanotubes parallel to the c-direction which are arranged hexagonally. The inner diameter of these nanotubes is around 5 Å. Both in between and inside the nanotubes there are sodium cations. Using the oxidation states of Na^+ and O^{2-} leads to a d^1 configuration for the vanadium atoms, all of which exhibit a square pyramidal coordination with short vanadyl bonds (1.63−1.64 Å). Thus the elementary building blocks of the V_3O_7 nanotubes are square pyramidal VO_5 units, and the lowest d level of vanadium, that is, the orbital bearing the unpaired electron, is the d_{xy} orbital (**1**). To analyze the magnetic interactions between these d_{xy} orbitals it is very important to correctly understand the different types of V−V interactions in the nanotubes.

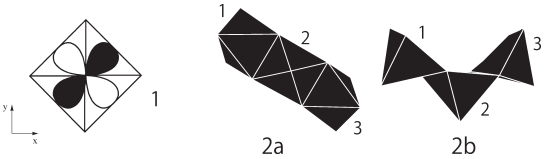

Three VO_5 square pyramids lead to a triply fused V_3O_{11} unit by sharing two edges as shown in **2** (**2a** is is a top view and **2b** a side view). There are three different vanadium atoms (for simplicity we label as 1, 2, and 3 the corresponding square pyramids in the structural diagrams) and two different V−V short distances within these units, 2.905 Å (V1−V2) and 3.062 Å (V2−V3). Three of these units can be condensed to form a V_9O_{27} ring **3** by sharing two edges per V_3O_{11} triple unit. In such way a total of three new short V−V short distances of 2.980 Å (V1−V3) are created. Thus, within a ring, all square pyramids share one edge with each of its nearest neighbors so that there are a total of nine V−V short distances (2.905 Å × 3, 3.062 Å × 3 and 2.980 Å × 3). Note that there are six additional V−V intra-ring interactions between VO_5 square pyramids which share just one oxygen atom. Three of them are of V2−V1 type (3.714 Å) and three of the V2−V3 type (3.574 Å). Thus there are five different types of short intra-ring V−V interactions, three associated with edge-sharing and two with corner-sharing square pyramids. The total number of short intra-ring V−V interactions per ring is thus 15.

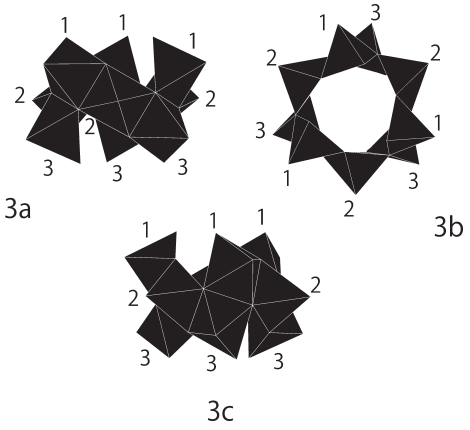

Two V_9O_{27} ring units **3**, one of which **(3c)** may be obtained from **(3a)** by the operation of a glide plane perpendicular to the ring, can be condensed through corner-sharing of six oxygen atoms as shown in **4**, leading to a $V_{18}O_{48}$ double ring. Through this process, 12 short inter-ring V−V distances are created. Three are of the V2−V1 type (3.357 Å), three are of the V3−V2 type (3.371 Å), and six of the V3−V1 type (3.493 × 3 Å and 3.610 × 3 Å). Thus, there are four different types of short inter-ring V−V interactions all of them associated with corner-sharing square pyramids. The total number of short inter-ring V−V interactions per double ring is thus 12.

The V_3O_7 nanotube **5** is obtained by successive condensation of these double rings through corner sharing of six oxygen atoms exactly as described for the generation of **4**. To summarize, the repeat unit of the nanotube is thus a $V_{18}O_{42}$ block, the number of different short V−V contacts ($d \leq 3.75$ Å) is nine, and the total number of those short V−V contacts is 42. The nine different short V−V contacts are those which have been taken into account in previous theoretical studies.[15−17] However, because of the special topology of the nanotube there are other V−V interactions that even if they are associated with longer V−V contacts are crucial in correctly understanding the magnetic interactions in this compound. The total number of different types of V−V interaction per

Table 1. Experimental and Calculated Coupling Constants (in cm^{-1}) for Four Hydroxo- and Alkoxo-Bridged Dinuclear V(IV) Compounds

compound	formula[a]	$J_{calc/PBE}$	$J_{calc/B3LYP}$	J_{exp}	ref.
A	$[(VO)_2(OH)_2([9]aneN_3)_2]^{2+}$	−544	−259	−354	51
B	$[VO(OCH_3)(ma)]_2$	−255	−84	−214	52
C	$[(VO)_2(cit)(Hcit)]^{3-}$	−674	−293	−424	53
D	$[(VO)_2(Hsabhea)(OCH_3)(HOCH_3)(acac)]$	+35.5	+15.4	+10.6	54

[a] Abbreviations: [9]aneN$_3$ = 1,4,7-triazacyclononane; H$_4$cit = citric acid; H$_3$sabhea = N-salicyclidene-2-[bis(2-hydroxyethyl)amino]ethylamine; Hacac = 2,4-pentanedione; ma = maltolato anion.

repeat unit which may be defined in the nanotube is 30 (vide infra, Figure 3).

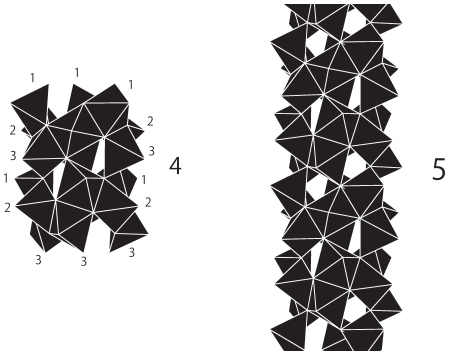

Testing the Computational Settings. To test the validity of our computational settings for this type of systems, we have computed first the exchange coupling constants for four molecular hydroxo- and alkoxo-bridged dinuclear V(IV) compounds using their corresponding crystal structures as obtained from the Cambridge Structural Database (CSD) with no further modeling. The results are collected in Table 1 along with the experimental values obtained from fitting of the magnetic susceptibility and the computed values obtained using a different computational setting.[22] Although the GGA functional (PBE) does not perform as well as the hybrid functional (B3LYP), the important observation is that it is able to reproduce the sign of all the coupling constants, that is, the antiferro- or ferromagnetic nature of the interactions, and their relative magnitudes.

Dimer Approximation and the Full Set of Coupling Constants. According to the previous results our computational settings should be able to reproduce the nature of the exchange interactions as well as their relative magnitude within the V(IV) oxide nanotube. As a first approximation, we have computed separately the 30 different coupling constants in the unit cell in a way which combines simplicity and precision. This will allow us to identify the most important coupling constants and, in the final accurate study, to neglect those that are predicted to be very small. To obtain each coupling constant, we substitute 16 out of the 18 paramagnetic V(IV) ions of the nanotube by 16 diamagnetic Ti(IV) ions, thus keeping the total charge of the system constant and leaving only 2 magnetic centers, that is, a single dimer in the unit cell, $V_2Ti_{16}O_{42}$. We have evaluated the coupling constant for each dimer as the difference between the high-spin (HS) state (a triplet in this case) and the low-spin (LS) state (a broken-symmetry or spin-polarized singlet). We have proceeded like this for each of the 30 coupling constants

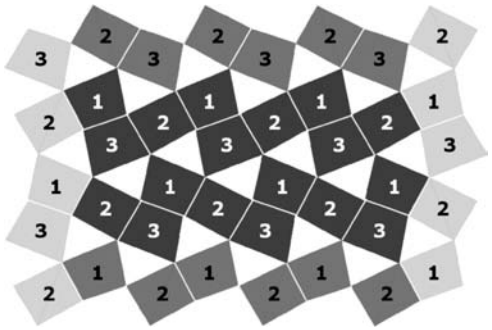

Figure 2. Different vanadium centers in the unfolded representation of the V_3O_7 nanotubes (see text): every vanadium center is classified as one of the three crystallographically different vanadium atoms of the original structural report.[1]

within the unit cell. This computational strategy, that is, the so-called dimer approximation,[55] which is based on the substitution of $n - 2$ paramagnetic ions by diamagnetic ones with the same charge, allows a first systematic approximation to the coupling constants in polynuclear systems. This scheme has been already used for tri-, tetra-, and hexanuclear Cu(II) and Ni(II) complexes with great success[21,25,56,57] and to the best of our knowledge is used here for the first time for an infinite system.

Labeling the different coupling constants in this system is easier if an unfolded representation of the nanotube is used. This is shown in Figure 2, where the different square pyramids are shown as more or less distorted rectangles. To facilitate the labeling of the different interactions, when dealing with interactions near the borders of these unfolded representations, we have added in these drawings a column of rectangles at the borders of these unfolded nanotubes (i.e., the clearer rectangles). The darker rectangles are the repeat unit of the nanotube. In Figure 2 we categorize each vanadium as one of the three crystallographically different vanadium atoms, using the

(51) Wieghardt, K.; Bossek, U.; Volckmar, K.; Swiridoff, W.; Weiss, J. *Inorg. Chem.* **1984**, *23*, 1387.
(52) Sun, Y.; Melchior, M.; Summers, D. A.; Thompson, R. C.; Rettig, S. J.; Orvig, C. *Inorg. Chem.* **1998**, *37*, 3119.
(53) Burojevic, S.; Shweky, I.; Bino, A.; Summers, D. A.; Thompson, R. C. *Inorg. Chim. Acta* **1996**, *251*, 75.
(54) Plass, W. *Angew. Chem., Int. Ed. Engl.* **1996**, *35*, 627.
(55) The so-called *dimer approximation*, as used here, was proposed in reference 56. After completion of our work, a comparative study of different ways to approximate the magnetic coupling constants has appeared (Bencini, A.; Totti, F., *J. Chem. Theory Comput*., **2009**, *5*, 144.) where this kind of approximation has been termed the doped cluster approach. All along our study we keep the original dimer approximation label to refer to it. Note that some care is needed when choosing the appropriate diamagnetic ions used to substitute the paramagnetic ones (for instance, orbital extension, etc.).
(56) Ruiz, E.; Rodriguez-Fortea, A.; Alemany, P.; Alvarez, S. *Polyhedron* **2001**, *20*, 1323.
(57) Ruiz, E.; Cano, J.; Alvarez, S.; Caneschi, A.; Gatteschi, D. *J. Am. Chem. Soc.* **2003**, *125*, 6791.

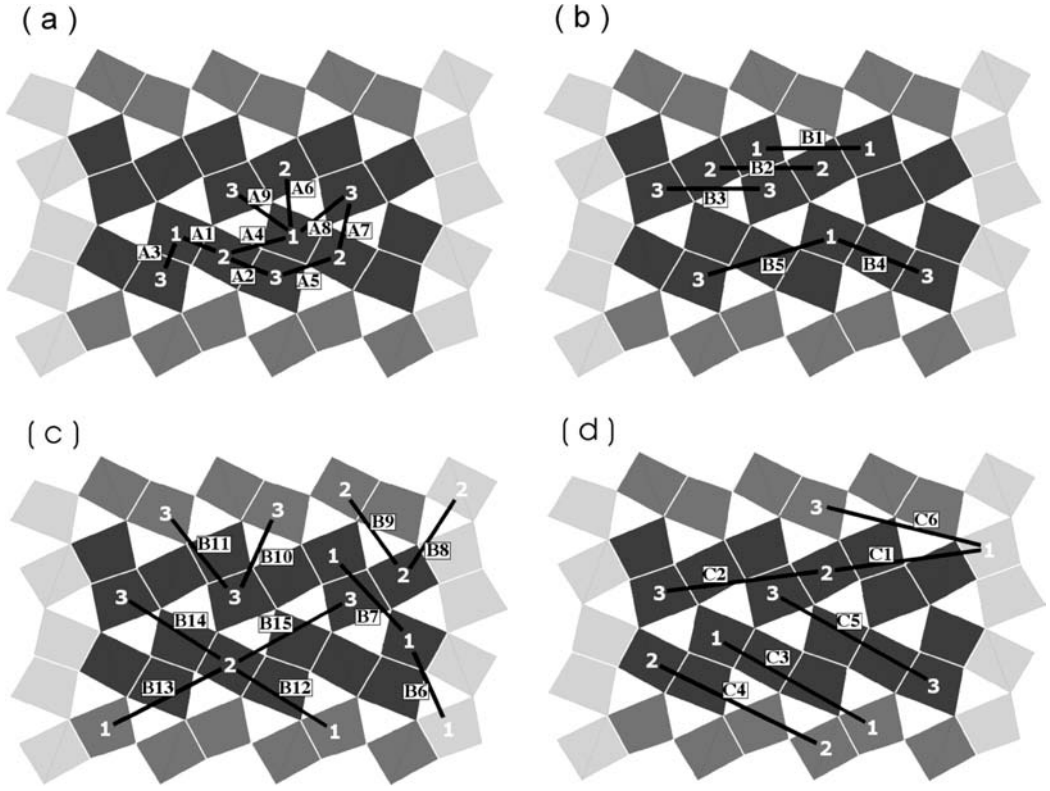

Figure 3. Labeling of the 30 different magnetic interactions (see text): (a) nearest-neighbors interactions, (b) intra-ring next-nearest-neighbors interactions, (c) inter-ring next-nearest-neighbors interactions, and (d) next-next-nearest-neighbors interactions.

same nomenclature as in the original structural report.[1] The labeling used for the different magnetic interactions is that illustrated in Figure 3, panels a−d. The JA*n* (n = 1−9) interactions are those associated with nearest-neighbors (NN). The JB*n* (n = 1−15) interactions are associated with next-nearest-neighbors (NNN) and can be separated in two different groups: those associated with intra-ring interactions (JB1−JB5) and those associated with inter-ring interactions (JB6−JB15). Finally, the interactions denoted as JC*n* (n = 1−6) are associated with next-next-nearest-neighbors. Because of the symmetry within the unit cell, there exists more than one combination of metallic centers to compute a given coupling constant. We have calculated all the possibilities and after checking that the differences among them were very small, that is, within the error of the calculation, we have averaged them.[58] Table 2 shows the averaged values for the 30 coupling constants evaluated within the *dimer approximation*.

In the following, by using the values obtained from the dimer approximation as a guide, we will first find out the set of N largest coupling constants which should be considered, and then compute the appropriate N + 1 spin states of the V_{18} nanotube. This will allow us to obtain their values without modeling the system (vide infra).

How Many Different Coupling Constants Are Needed to Describe the System? Looking at the results of Table 2, we observe that the largest coupling constants mostly coincide with the nine interactions between nearest-neighbor (NN) V(IV) ions. However, there are some notable exceptions. For example, JA2, which corresponds to a NN interaction, is predicted to be very small (1.5 cm^{-1}) whereas JB1, which corresponds to a NNN interaction, is predicted to be moderately antiferromagnetic (−63 cm^{-1}). Moreover, other interactions that have not been considered in the theoretical studies published so far, as for example the NNN interactions described by JB3, JB4, and JB5, which also show moderate antiferromagnetic behavior, may play an important role in determining the magnetic properties of the present V(IV) oxide nanotube. The rest of NNN interactions (JB2, JB6−JB15) and the next-next-nearest-neighbor (NNNN) interactions (JC2−JC6) are smaller. Once we have used the dimer model to obtain an evaluation of all 30 coupling constants, we propose a systematic procedure to determine the minimal set of constants that should be included in any sensible model for the magnetic interactions in this compound. For this purpose we consider different sets with a decreasing number of coupling constants (obtained by neglecting the smallest ones) and examine what is the minimal set for which *both* the density of states (DOS) for all the possible spin configurations *and* the ground state are stable. Following this procedure, we have computed the DOS for all the 2^{18} possible spin configurations using three different sets of constants. Figure 4 displays the

(58) Note that we are using periodic boundary conditions and a unit cell with sixty atoms ($V_{18}O_{42}$), i.e., two rings. This means that when calculating interactions as for instance JB5 associated with V3 and V1 within the unit cell, the calculated constant includes also the coupling of V3 within the cell and the periodic copies of V1 outside the cell. To separate these added contributions larger unit cells should be used. However, these "additional" contributions are very small and have practically no influence on the results. Also note that interactions like those associated with one atom of the $V_{18}O_{42}$ unit cell and those which are equivalent by translation are not taken into account except if using larger unit cells. Again, these interactions are very small and practically do not affect the results.

DOS computed using the largest 9, 12, and the complete set of 30 coupling constants.

The DOS computed using only the largest 9 *J*'s does not match that obtained considering all 30 *J*'s (see Figure 4). Moreover, the predicted lowest-energy collinear spin configuration is different from that predicted with all 30 *J*'s. The largest 9 *J*'s include the 8 NN coupling constants plus the interaction corresponding to JB1.

Table 2. Values for the 30 Coupling Constants (in cm^{-1}) Evaluated within the *Dimer Approximation* along with the Type of Interaction That Represents Each Coupling Constant[a]

interaction	coupling constant	type
JA1	−75.2	NNe
JA2	1.5	NNe
JA3	−117.8	NNe
JA4	−195.5	NNc
JA5	−130.0	NNc
JA6	73.2	NNc
JA7	92.6	NNc
JA8	174.2	NNc
JA9	121.4	NNc
JB1	−62.9	NNN
JB2	−9.5	NNN
JB3	−29.8	NNN
JB4	−28.4	NNN
JB5	−43.4	NNN
JB6	10.4	NNN
JB7	15.7	NNN
JB8	4.4	NNN
JB9	10.8	NNN
JB10	4.2	NNN
JB11	14.5	NNN
JB12	0.6	NNN
JB13	4.1	NNN
JB14	5.3	NNN
JB15	5.1	NNN
JC1	−13.0	NNNN
JC2	−6.6	NNNN
JC3	−3.8	NNNN
JC4	−1.8	NNNN
JC5	−4.3	NNNN
JC6	0.6	NNNN

[a] NN: nearest-neighbors, NNN: next-nearest-neighbors, and nex-next-nearest-neighbors; c: corner-sharing, e: edge-sharing.

The DOS computed when the largest 12 *J*'s are taken into account (8 NN + 4 NNN) matches almost perfectly the distribution obtained with all 30 *J*'s. The predicted lowest-energy collinear spin state is also the same. Therefore, *within the dimer approximation, the magnetic properties of the nanotubular system seem to be well converged when the largest 12 J's are taken into consideration*.

Beyond the Dimer Approximation. According to these results, we have computed the same 12 coupling constants from the V_{18} non-modeled system. The results are shown in the third column of Table 3.

The 12 coupling constants obtained in such way are smaller in their magnitudes than those computed with the dimer approximation. However, the signs of the coupling constants, that is, the nature of the exchange interaction, are all the same except for one case, JB5. Moreover, the relative magnitude of the different *J* values is the same with the two methodologies. There are four moderately large ferromagnetic interactions (JA8, JA9, JA6, JA7) and four moderately large antiferromagnetic interactions (JA4, JA1, JA5, JA3). These eight largest coupling constants all correspond to NN interactions. As for the four

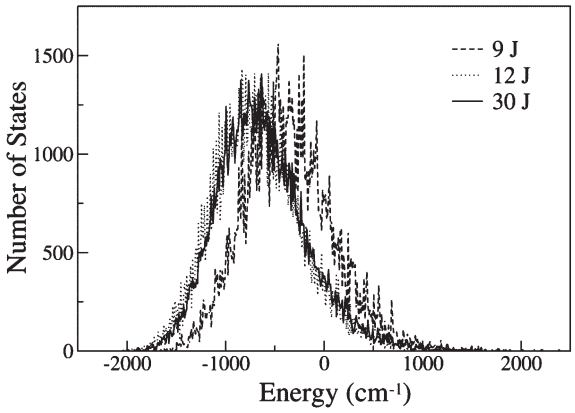

Figure 4. DOS for all the 2^{18} possible spin configurations computed considering the largest 9, 12, or the total 30 coupling constants obtained from the dimer approximation. The zero energy corresponds to the ferromagnetic state ($S = 18/2$).

Table 3. Values for the Coupling Constants (in cm^{-1}) Evaluated Using Different Approximations (V_2Ti_{16} or V_{18}) along with the Most Significant Structural Parameters Involved in the Interactions

interaction	17 J_{V18}	12 J_{V18}	J_{dimer}	type[a]	d_{VV} (Å)	VOV (deg)	δ (deg)[c]	τ (deg)[d]
JA1	−62.1	−64.4	−75.2	NNe	2.905	99.6[b]	44.2	9.1
JA3	−39.5	−25.7	−117.8	NNe	2.980	99.4[b]	42.3	25.1
JA4	−99.3	−97.9	−195.5	NNc	3.714	142.4	77.8	17.7
JA5	−40.7	−55.1	−130.0	NNc	3.547	136.0	76.5	20.7
JA6	76.6	70.2	73.2	NNc	3.357	117.6	21.2	17.8
JA7	75.9	91.2	92.6	NNc	3.371	120.5	21.1	16.6
JA8	163.3	154.5	174.2	NNc	3.493	133.6	64.6	57.1
JA9	84.7	88.2	121.4	NNc	3.610	132.0	65.1	56.8
JB1	−24.7	−2.9	−62.9	NNN	5.197			
JB3	−15.0	−9.2	−29.8	NNN	5.180			
JB4	−15.4	−37.8	−28.4	NNN	5.522			
JB5	−4.7	8.4	−43.4	NNN	6.248			
JB6	21.1		10.4	NNN	5.242			
JB7	13.6		15.7	NNN	6.070			
JB9	15.0		10.8	NNN	5.680			
JB11	0.3		14.5	NNN	5.985			
JC1	−7.1		−13.0	NNNN	6.123			

[a] The nearest-neighbors (NN) interactions are divided in two groups: edge-sharing (edge) and corner-sharing (corner). [b] Average value of the two V−O−V angles. [c] Angle between the two VO_{apical} vectors. [d] OVVO dihedral angle.

important NNN interactions, the predictions obtained from the V_{18} non-modeled system show much smaller but still non-negligible values, except for JB4. In general, the discrepancy between the two methodologies is more important for the antiferromagnetic couplings (vide infra).

Structural Rationalization of the Nearest-Neighbors Coupling Constants. The values for the coupling constants corresponding to the NN interactions can be rationalized with the aid of the different structural parameters involved in the interactions. The coupling constants for the two edge-sharing interactions (JA3, JA1) are negative but not very large, that is, they indicate moderate antiferromagnetic interactions. According to the classification given by Plass,[54] in these interactions the V(IV) ions are arranged in a syn-orthogonal configuration. The coupling constants for hydroxo- and alkoxo-bridged dinuclear V(IV) compounds with V···V distances smaller than 3 Å and VOV angles less than 100° are large and negative (see **A**, **B**, and **C** in Table 1) as a consequence of the direct σ overlap between the metal orbitals that bear the unpaired electron (through-space exchange).[22] The smaller values obtained for JA3, JA1 are associated with the loss of planarity in the syn-orthogonal configuration, as a consequence of the unusual geometry of the nanotube (42.3 and 44.2°, respectively, for the angle between the VO_{apical} vectors, δ). This loss of planarity induces a loss of overlap between the orbitals that bear the unpaired electron, **6**, and hence a weakening of the exchange interaction. For the remaining edge-sharing NN coupling constant (JA2), which cannot be found within the largest 12 J's, an increase of the V···V distance to 3.062 Å (with an angle of 45.3° between the VO_{apical} vectors) is the main reason for the very small coupling constant, but a compensation between ferromagnetic and antiferromagnetic contributions ($J = J_{FE} + J_{AF}$)[59] also plays some role.

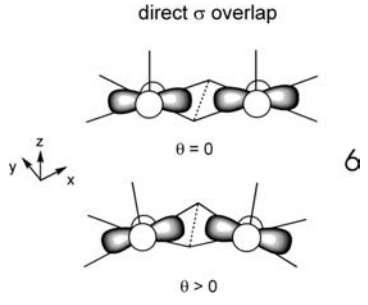

The coupling constants for NN corner-sharing interactions are antiferromagnetic (JA4, JA5) or ferromagnetic (JA6, JA7, JA8, JA9) depending on the structural parameters involved. For corner-sharing interactions, the exchange interaction is transmitted by the superexchange mechanism through the orbitals of the bridging oxygen atom. In these cases, the V−O−V angle becomes an important structural parameter to understand the nature of the coupling, **7**. The antiferromagnetic interactions (JA4, JA5) are related to larger VOV angles than those featured by the ferromagnetic interactions (JA6, JA7, JA8, JA9): the larger the VOV angle the larger the π overlap between the metal orbitals that bear the unpaired electron and the p orbital of the oxo bridging ligand, thus increasing the antiferromagnetic interaction. The smallest VOV angles correspond to the JA6 and JA7 interactions (117.6 and 120.5°, respectively), but the values associated with these interactions are not as large as those for JA8 and JA9. The interactions corresponding to these later constants are associated with large deviations from coplanarity of the two adjacent VO_4 planes. Not only is the angle between the two VO vectors very large (around 65°), but also the large dihedral OVVO angle leads to a larger orthogonality, that is, a much worse overlap between orbitals through the bridge, **8**. Experimental results in ball-shaped polyoxovanadates show that single μ_3-O bridges are able to mediate antiferro- or ferromagnetic interactions depending on the structural parameters of the bridge or the coordination sphere around the V(IV) centers.[60,61] In particular, similar strong ferromagnetic interactions mediated by single μ_3-O bridges in which the two VO_4 planes are almost orthogonal have been reported for a ball-shaped octanuclear polyoxovanadate.[61]

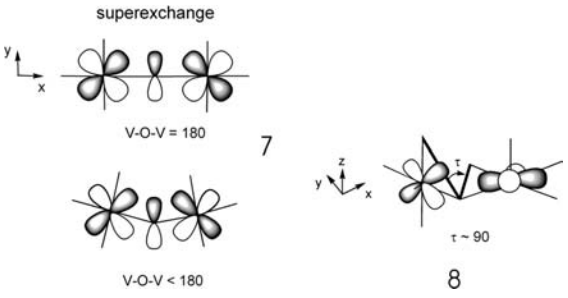

Lowest-Energy Collinear Spin Configuration. From the values obtained so far for the exchange coupling constants, we observe that all the large antiferromagnetic interactions are found within each nine-member ring of the nanotube (intra-ring) whereas all the large ferromagnetic couplings are found between the two rings within the unit cell (inter-ring) in agreement with the work of Mazurenko et al.[17] As a result, we will find situations in which the spins at some V(IV) centers are frustrated. The lowest-energy collinear spin configuration predicted by the chosen set of 12 J's is the same as that predicted within the dimer approximation. The total spin is zero, that is, it is a spin-polarized singlet. A set of six equivalent spin configurations with total $M_S = 1$ lay 86 cm^{-1} above. Analyzing the lowest-energy collinear spin configuration (Figure 5), we observe that ferromagnetic interactions between the atoms of two different rings (inter-ring) exist because of the large positive values of JA8 and JA9. As a consequence, the ferromagnetic interaction associated to JA7 is frustrated. Within the rings (intra-ring), there are some antiferromagnetic interactions between some V(IV) ions (V2−V1) whereas some other interactions are ferromagnetic (V2−V3) thus frustrating the antiferromagnetic

(59) Kahn, O. *Molecular Magnetism*; VCH: New York, **1993**.

(60) Muller, A.; Sessoli, R.; Krickemeyer, E.; Bogge, H.; Meyer, J.; Gatteschi, D.; Pardi, L.; Westphal, J.; Hovemeier, K.; Rohlfing, R.; Doring, J.; Hellweg, F.; Beugholt, C.; Schmidtmann, M. *Inorg. Chem.* **1997**, *36*, 5239.

(61) Hegetschweiler, K.; Morgenstern, B.; Zubieta, J.; Hagrman, P. J.; Lima, N.; Sessoli, R.; Totti, F. *Angew. Chem., Int. Ed.* **2004**, *43*, 3436.

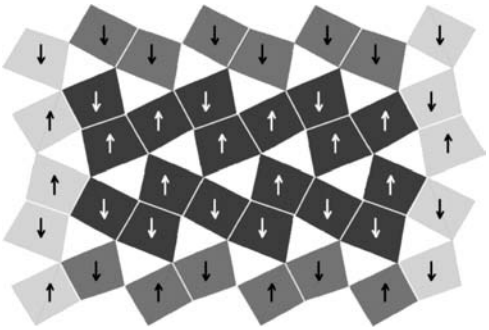

Figure 5. Schematic representation of the lowest-energy collinear spin configuration.[62]

interaction associated to JA5. So, for each ring there is a total $|M_S| = 3/2$ value with different sign that is compensated to yield the singlet lowest-energy collinear spin configuration.

Shown in Figure 6a is the band structure calculated for this state. Every band in Figure 6a is really the superposition of two bands, one with alpha spin and the other with beta spin. The bands labeled with an asterisk are pairs of e-type symmetry bands at Γ whereas the others are of a-type symmetry. Thus, there are two groups of nine alpha spin bands and nine beta spin bands with the d_{xy} orbitals of the vanadium atoms as their major components, filled with the 18 d electrons per repeat unit of the system. We found an electronic gap of 0.95 eV separating the top of these d_{xy} bands from the next d levels, in good qualitative agreement with the occurrence of a broad 1.2 eV band in the experimental absorption spectrum of $Na_2V_3O_7$. Despite the well-known problems of DFT in reproducing optical gaps, we believe that this fact provides a basis for the previous attribution[9] of this feature to a vanadium d → d transition. Mazurenko et al.[17] calculated very similar electronic energy gaps, 1.14 and 1.18 eV, although they used the LDA + U approach and two different collinear magnetic configurations which according to our calculations are 1359 and 1522 cm^{-1} higher in energy than that of Figure 5. Shown in Figure 6, panels b and c, are the partial DOS curves associated with the vanadium atoms of two successive V_9O_{27} rings (black lines), as well as the contributions of the three different types of vanadium atoms. The three lowest pairs of bands are mostly built from the V3 and V2 d_{xy} orbitals but those of V3 dominate. The V1 contribution dominates in the upper bands, although with only one exception, there is a more extensive mixing between the d_{xy} orbitals of the three different sites in these levels. The dominance of the d_{xy} orbital of V3 in the lower levels and that of V1 in the upper ones is mostly a consequence of the progressive increase from V3 to V1 of the antibonding interactions of the vanadium d_{xy} orbital with the basal oxygen atoms. For instance, the average $V-O_{basal}$ distance decreases from 1.972 Å for V3 to 1.946 Å for V2 and 1.919 Å for V1, so that the stability of the associated d_{xy} orbital decrease in the same order.

(62) The collinear spin ground state for this system is a combination of two equivalent lowest-energy collinear spin configurations: that sketched in figure 5 and the equivalent one in which the values of the m_s for each V(IV) center are inverted.

When Should Additional Couplings Be Considered? The set of 12 coupling constants in the complete V_{18} system predicts the same lowest-energy collinear spin configuration as that predicted within the V_2Ti_{16} dimer approximation, and it provides meaningful values for the NN coupling constants according to the structural parameters of the bridging ligands and of the coordination sphere of the magnetic centers. The values obtained for the NNN coupling constants, however, do not match so satisfactorily those obtained within the dimer approximation. The absolute deviation is not very different from that observed for the NN interactions, but their smaller values lead to a different prediction concerning the nature of the interaction, that is, of the sign of the coupling constant, depending on the approximation used. Several factors can be at the origin of this discrepancy: (a) the use of a reduced set (12) of coupling constants, and (b) the appropriateness of the dimer approximation. The latter point will be discussed in the next section; let us now consider the first point.

The coupling constants that we neglect are predicted to be small within the dimer approximation, but there is a large number of them, that is, a total of 18. Therefore, the fitting of the computed energies for the different spin configurations to 12 *J*'s includes in average the effect of the 18 neglected constants. This drawback will of course be reduced if more constants are included explicitly in the model. If we neglect the 13 constants that are smaller than 10 cm^{-1} within the dimer approximation, which are expected to be very small (within the error of our methodology), a total of 17 exchange parameters remain. Moreover, if these very small constants were included in a model for the magnetic coupling in this compound, there would be no reason to neglect constants that couple paramagnetic centers on different cells, leading to an over parametrization of the system.[58] Now, for this set of 17 *J*'s, the signs of the constants are calculated to be in agreement with those of the dimer approximation. Moreover, the values obtained for the larger NN coupling constants are very similar to those found using the set of 12 *J*'s and the values for the other constants (8 NNN + 1 NNNN) match correctly those of the dimer approximation. The lowest-energy collinear spin configuration is computed to be the same as that predicted for the set of 12 *J*'s. We have also computed the DOS using the two sets of solutions (12 and 17 *J*'s, see Figure 7). Apart from predicting the same three lowest-energy configurations, their DOS curves match almost perfectly in energy range, as well as in the number of states. Therefore, we can conclude that the small set of 12 *J*'s is able to reproduce the predictions made by the more complete set of 17 *J*'s, albeit the smaller coupling constants do not compare so well with those obtained with the dimer approximation. The effect of including more coupling constants in the fitting procedure allows for a much better matching with those constants obtained with the dimer approximation because the effect of the neglected constants is smaller.

Validity of the Dimer Approximation. The last point we would like to address is the validity of the dimer approximation. Although we have shown that it is an excellent way to detect the important exchange interactions in

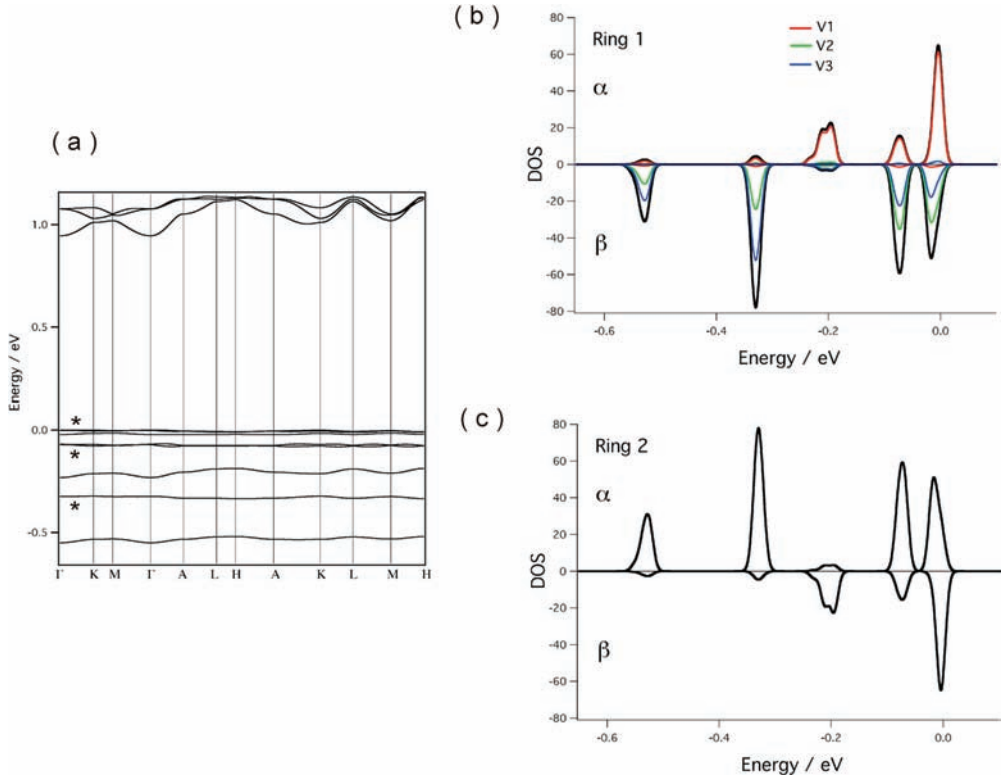

Figure 6. Band structure (a) and projected DOS of the vanadium atoms of two successive rings (b) and (c) in the lowest-energy collinear spin configuration. In panel b are shown the projections corresponding to the three different types of vanadium atoms. The labeling of the vanadium atoms is the same used in Figure 2 and corresponds to that used for crystal structure determination.[1] The energy zero has been taken to be that of the top occupied level.

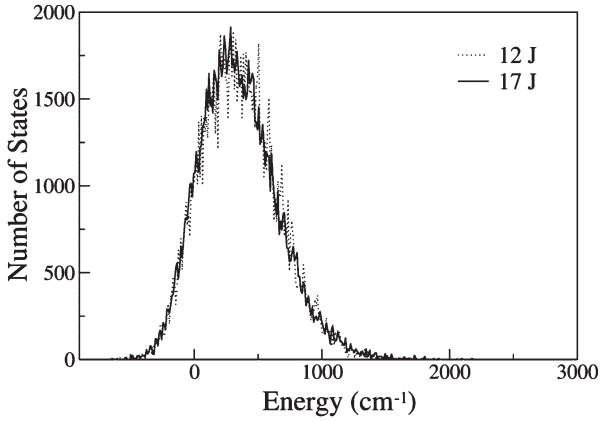

Figure 7. DOS for the 2^{18} possible spin configurations computed considering the largest 12 and 17 coupling constants obtained from fitting to the computed values of the complete V_{18} nanotube. The zero energy corresponds to the ferromagnetic state ($S = 18/2$).

complex systems, an important question remains open: will the value of the coupling constants fitted from the computed energies in the V_{18} nanotube converge to the value predicted from the dimer approximation if all 30 J's are considered in the model? The answer is no. Comparing the DOS computed for the V_{18} system (Figure 7) with that obtained for the V_2Ti_{16} model (Figure 4), we observe that their shapes are very similar, but those corresponding to the V_2Ti_{16} model are shifted to more negative values (the maximum of the curve is between -500 and -1000 cm^{-1}) than those for the V_{18} system (the maximum lies around $+300$ or $+400$ cm^{-1}). This is a consequence of the overestimation of the antiferromagnetic interactions in the dimer approximation. To assess this point, we have computed some large NN coupling constants corresponding to ferro- and antiferromagnetic interactions with a V_3Ti_{15} model to understand the effect of increasing the number of paramagnetic centers. We have first computed (JB1, JA1, JA4) considering a trimer and then (JA8, JA9, JB3) using a different trimer. The results are collected in Table 4.

Table 4. Values for Selected Coupling Constants (in cm^{-1}) Evaluated Using Different Approximations: V_2Ti_{16}, V_3Ti_{15}, and V_{18} (17J)[a]

interaction	V_2Ti_{16}	V_3Ti_{15}	V_{18} (17J)
JA1	−75.2	−54.1	−62.1
JA4	−195.5	−176.6	−99.3
JA8	174.2	171.3	163.3
JA9	121.4	112.9	84.7
JB1	−62.9	−39.1	−24.7
JB3	−29.8	−26.0	−15.0

[a] The model with all paramagnetic atoms and a set of 17 relevant coupling constants.

The antiferromagnetic coupling constants computed for V_2Ti_{16} are more negative (overestimated) than those computed for V_3Ti_{15} or for V_{18} (17J). The values for V_3Ti_{15} are, in general, between those obtained for V_2Ti_{16} and V_{18} (17J), except for JA1. The variation in the ferromagnetic coupling constants is much smaller. Similar results were also reported for hydroxo-bridged trinuclear Cu(II) complexes: the antiferromagnetic coupling constants computed for the model Cu_2Zn, in which one Cu(II) ion is substituted by one diamagnetic Zn(II) ion, were more negative than those obtained for the Cu_3 trimer. As in the present study, the ferromagnetic coupling constants were not so much affected.[21]

Concluding Remarks

The electronic structure and spin exchange interactions in the vanadium(IV) oxide $Na_2V_3O_7$ nanotubes have been studied by means of DFT calculations within the GGA approximation. Concerning the exchange interactions, this system is far from being trivial to analyze because it presents as much as 30 different exchange interactions in the unit cell. This is the first time that all the important coupling constants of this system have been computed directly from the energy differences of several spin configurations. We have found that estimating the coupling constants using the dimer approximation, that is, using an appropriate V_2Ti_{16} model for each constant, albeit overestimating the antiferromagnetic interactions, provides for important qualitative information. The relative magnitude of the different interactions (important vs negligible coupling constants), the nature of their magnetic coupling (especially for large coupling constants), and even the prediction of the lowest-energy collinear spin configuration are possible using a set of V_2Ti_{16} models. To get more quantitative results, the coupling constants should be obtained from the computed energies of the complete system, V_{18} in the present case. The values calculated from the dimer approximation are a simple way to discriminate among the coupling constants and to select the set of most important ones.

Because of the peculiar geometry of the nanotube, the NN coupling constants are not found to be the only important ones as assumed in previous studies. Other NNN interactions cannot be neglected to obtain a proper description of the magnetic properties of the system. Previous studies of the magnetic interactions in $Na_2V_3O_7$ are found to be incorrect with the exception of the work of Mazurenko et al.[17] which is in qualitative agreement with the present results. We have found that the set of the 12 largest coupling constants is able to predict the lowest-energy collinear spin configuration. To get more meaningful values for the smaller coupling constants a larger set of at least 17 J's is necessary. In the lowest-energy collinear spin configuration, there is a ferromagnetic coupling between the rings (inter-ring) of the nanotube whereas the coupling can be ferro- or antiferromagnetic within the rings (intra-ring), resulting in two important spin frustrated interactions.

Because of the peculiar geometry imposed by the tubular structure, the correlation between the structure and the strength of the different coupling constants is somewhat involved. However, the main coupling constants follow these trends: (a) the coupling constants for edge-sharing interactions are moderate and antiferromagnetic as a result of the loss of σ-overlap between the V d_{xy} orbitals through the shared edge, something resulting from the loss of planarity imposed by the tubular shape; (b) for corner-sharing interactions the coupling may be ferro or antiferromagnetic mostly depending on the V−O−V angle: large angles favor an antiferromagnetic coupling, whereas small angles and large dihedral O−V−V−O angles favor ferromagnetic couplings.

Finally, let us note that our procedure can be used to analyze the magnetic properties of similar non-trivial periodic systems with many paramagnetic centers. If calculations for the spin states of the total system are not possible, the dimer approximation is able to provide at least useful qualitative information on the magnetic properties of the system.

Acknowledgment. We are indebted with Jorge Íñiguez for enlightening discussions concerning the magnetic behavior and nature of the ground state of $Na_2V_3O_7$. This work was supported by DGES-Spain (Projects FIS2006-12117-C04-01, CSD2007-00041, CTQ2008-06549-C02-01/BQU and CTQ2008-06670-C02-02/BQU) and Generalitat de Catalunya (Projects 2005 SGR 683, 2005SGR-00104 and 2005 SGR 00036). A.R.-F. and M. Ll. acknowledge support through the Ramón y Cajal program. Part of the computations described in this work were carried out using the facilities of CESCA.